

Topochemical Dihydrogen to Covalent Bonding Transformation in $\text{LiBH}_4 \cdot \text{TEA}$: A Mechanistic Study

Radu Custelcean* and James E. Jackson*

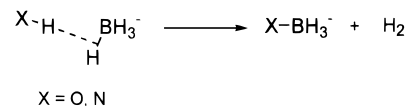
Contribution from the Department of Chemistry, Michigan State University, East Lansing, Michigan 48824-1322

Received December 13, 1999

Abstract: The first mechanistic investigation of a topochemical dihydrogen to covalent bonding conversion is presented. Solid-state decomposition of the $\text{LiBH}_4 \cdot \text{TEA}$ (TEA = triethanolamine) dihydrogen-bonded complex into a covalent material was studied using ^{11}B solid-state MAS NMR, FT-IR, XRD, and optical microscopy. The majority of this solid-state reaction occurs by nucleation and two-dimensional growth of the covalent product nuclei. Variable-temperature kinetics and H/D exchange experiments established that proton transfer between the OH groups of the TEA and the BH_4^- anions, at the reactant/product interface, is the rate-limiting step, with an associated activation barrier of 21.0 ± 2.4 kcal/mol. The activation parameters ΔH^\ddagger and ΔS^\ddagger for the same process were calculated to be 20.1 ± 2.4 kcal/mol and -16.8 ± 6.2 eu, respectively, comparable with the analogous values found for the aqueous hydrolysis of BH_4^- in neutral water, suggesting similar mechanisms for the solid and solution decompositions.

Dihydrogen bonding has long been recognized as a Lewis acid–base interaction between hydridic hydrogens of $\text{M}-\text{H}$ ($\text{M} = \text{B}, \text{Ga}, \text{Ir}, \text{Mo}, \text{Mn}, \text{Os}, \text{Re}, \text{Ru}, \text{W}$) bonds and traditional $\text{X}-\text{H}$ ($\text{X} = \text{O}, \text{N}, \text{F}, \text{C}$) proton donors.¹ A detailed structural and energetic characterization of these unconventional hydrogen bonds was achieved with the help of IR and NMR spectroscopy in solution,² X-ray or neutron diffraction in the solid state,³ and theoretical calculations in the gas phase.⁴ Recent experimental and theoretical studies with an emphasis on the reactivity and

Scheme 1



the implications of dihydrogen bonding in proton transfer have also been reported.⁵

The significance of this unusual and interesting interaction extends, however, beyond its fundamental aspects. With strength and directionality comparable with those found in conventional hydrogen bonding, dihydrogen bonds can serve as organizing interactions to guide chemical reactions. Very recently we exploited dihydrogen bonds to control reactivity and diastereoselectivity of borohydride reductions of α -hydroxyketones in solution.⁶ Additionally, dihydrogen bonds, like conventional hydrogen bonds, can serve as control elements in crystal engineering.⁷ But unlike the classical kind, dihydrogen bonds can topochemically react in the solid by H_2 loss, exchanging the weak $\text{H} \cdots \text{H}$ interactions for strong covalent bonds (Scheme 1), and thus opening new routes to the rational assembly of ordered, extended covalent materials.⁸

Our initial efforts toward the topochemical assembly of covalent materials using dihydrogen bonds have concentrated

(1) (a) Brown, M. P.; Heseltine, R. W.; Smith, P. A.; Walker, P. J. *J. Chem. Soc. A* **1970**, 983. (b) Stevens, R. C.; Bau, R.; Milstein, D.; Blum, O.; Koetzle, T. F. *J. Chem. Soc., Dalton Trans.* **1990**, 1429. (c) Lough, A. J.; Park, S.; Ramachandran, R.; Morris, R. H. *J. Am. Chem. Soc.* **1994**, *116*, 8356. (d) Crabtree, R. H.; Siegbahn, P. E. M.; Eisenstein, O.; Rheingold, A. L.; Koetzle, T. F. *Acc. Chem. Res.* **1996**, *29*, 348. (e) Shubina, E. S.; Belkova, N. V.; Epstein, L. M. *J. Organomet. Chem.* **1997**, *536*–537, 17. (f) Alkorta, I.; Rozas, I.; Elguero, J. *Chem. Soc. Rev.* **1998**, *27*, 163. (g) Braga, D.; De Leonardi, P.; Grepioni, F.; Tedesco, E.; Calhorda, M. J. *Inorg. Chem.* **1998**, *37*, 3337.

(2) (a) Peris, E.; Lee, J. C.; Rambo, J. R.; Eisenstein, O.; Crabtree, R. H. *J. Am. Chem. Soc.* **1995**, *117*, 3485. (b) Shubina, E. S.; Belkova, N. V.; Krylov, A. N.; Vorontsov, E. V.; Epstein, L. M.; Gusev, D. G.; Niedermann, M.; Berke, H. *J. Am. Chem. Soc.* **1996**, *118*, 1105. (c) Epstein, L. M.; Shubina, E. S.; Bakhmutova, E. V.; Saitkulova, L. N.; Bakhmutov, V. I.; Chistyakov, A. L.; Stankevich, I. V. *Inorg. Chem.* **1998**, *37*, 3013.

(3) (a) Wessel, J.; Lee, J. C.; Peris, E.; Yap, G. P. A.; Fortin, J. B.; Ricci, J. S.; Sini, G.; Albinati, A.; Koetzle, T. F.; Eisenstein, O.; Rheingold, A. L.; Crabtree, R. H. *Angew. Chem., Int. Ed. Engl.* **1995**, *34*, 2507. (b) Patel, B. P.; Yao, W.; Yap, G. P. A.; Rheingold, A. L.; Crabtree, R. H. *Chem. Commun.* **1996**, 991. (c) Abdur-Rashid, K.; Gusev, D. G.; Landau, S. E.; Lough, A. J.; Morris, R. H. *J. Am. Chem. Soc.* **1998**, *120*, 11826. (d) Gusev, D. G.; Lough, A. J.; Morris, R. H. *J. Am. Chem. Soc.* **1998**, *120*, 13138. (e) Huang, L. Y.; Aulwurm, U. R.; Heinemann, F. W.; Knoch, F.; Kisch, H. *Chem. Eur. J.* **1998**, *4*, 1641. (f) Braga, D.; Grepioni, F.; Tedesco, E.; Calhorda, M. J.; Lopes, P. E. M. *New J. Chem.* **1999**, 219. (g) Abramov, Y. A.; Brammer, L.; Klooster, W. T.; Bullock, R. M. *Inorg. Chem.* **1998**, *37*, 6317.

(4) (a) Liu, Q.; Hoffmann, R. *J. Am. Chem. Soc.* **1995**, *117*, 10108. (b) Foces-Foces, C.; Elguero, J.; Alkorta, I. *Chem. Commun.* **1996**, 1633. (c) Gladfelter, W. L.; Cramer, C. J. *Inorg. Chem.* **1997**, *36*, 5358. (d) Popelier, P. L. A. *J. Phys. Chem. A* **1998**, *102*, 1873. (e) Scheiner, S.; Orlova, G. *J. Phys. Chem. A* **1998**, *102*, 260. (f) Scheiner, S.; Orlova, G. *J. Phys. Chem. A* **1998**, *102*, 4831. (g) Remko, M. *Mol. Phys.* **1998**, *94*, 839. (h) Petterson, M.; Lundell, J. *Phys. Chem. Chem. Phys.* **1999**, *1*, 1601.

(5) (a) Lee, J. C.; Peris, E.; Rheingold, A. L.; Crabtree, R. H. *J. Am. Chem. Soc.* **1994**, *116*, 11014. (b) Ayllon, J. A.; Gervaux, C.; Sabo-Etienne, S.; Chaudret, B. *Organometallics* **1997**, *16*, 2000. (c) Aime, S.; Gobetto, R.; Valls, E. *Organometallics* **1997**, *16*, 5140. (d) Guari, Y.; Ayllon, J. A.; Sabo-Etienne, S.; Chaudret, B. *Inorg. Chem.* **1998**, *37*, 640. (e) Chu, H. S.; Lau, C. P.; Wong, K. Y. *Organometallics* **1998**, *17*, 2768. (f) Cabalero, A.; Jalon, F. A.; Manzano, B. R. *Chem. Commun.* **1998**, 1879. (g) Orlova, G.; Scheiner, S.; Kar, T. *J. Phys. Chem.* **1999**, *103*, 514. (h) Grundemann, S.; Ulrich, S.; Limbach, H. H.; Golubev, N. S.; Denisov, G. S.; Epstein, L. M.; Sabo-Etienne, S.; Chaudret, B. *Inorg. Chem.* **1999**, *38*, 2550.

(6) Gatling, S.; Jackson, J. E. *J. Am. Chem. Soc.* **1999**, *121*, 8655.

(7) Campbell, J. P.; Hwang, J. W.; Young, V. G.; Von Dreele, R. B.; Cramer, C. J.; Gladfelter, W. L. *J. Am. Chem. Soc.* **1998**, *120*, 521.

(8) (a) Custelcean, R.; Jackson, J. E. *J. Am. Chem. Soc.* **1998**, *120*, 12935. (b) Custelcean, R.; Jackson, J. E. *Angew. Chem., Int. Ed. Engl.* **1999**, *38*, 1661. (c) Hwang, J. W.; Campbell, J. P.; Kozubowski, J.; Hanson, S. A.; Evans, J. F.; Gladfelter, W. L. *Chem. Mater.* **1995**, *7*, 517.

on the investigation of solid-state structures and reactivities of triethanolamine (TEA) complexes with various metal borohydrides ($\text{MBH}_3\text{X}\cdot\text{TEA}$; $\text{M} = \text{Na}, \text{Li}$; $\text{X} = \text{H}, \text{CN}$).^{8a,b} A few key factors such as the relative acidity and basicity of the protonic and hydridic partners and the melting points of these dihydrogen-bonded complexes were recognized to be critical for the solid-state chemistry of these systems. Now that the topochemical assembly of covalent solids from dihydrogen-bonded systems appears to be a viable concept, unlimited applications of this new strategy are conceivable, offering access to novel covalent materials with targeted structures and properties.

We seek a detailed understanding of the mechanism of these topochemical bond-forming processes. In the complex $\text{LiBH}_4\cdot\text{TEA}$ (**1**), strong complexation by the Li^+ ions significantly enhances the acidity of the OH groups, leading to extremely short $\text{H}\cdots\text{H}$ contacts and high solid-state reactivity. This fact, together with the high melting point of **1**, allowed a detailed study of this dihydrogen-bonded system and its topochemical decomposition. The present report describes our results from the systematic investigation of the solid-state decomposition of **1**, with the aim of probing the mechanism of this topochemical process both at the macroscopic and the molecular levels.

Results and Discussion

Solid-State Decomposition of $\text{LiBH}_4\cdot\text{TEA}$ (1**). A. General Characterization.** The synthesis and solid-state structure of **1**, as well as a succinct description of its decomposition, have been previously reported.^{8b} The crystal structure of **1** consists of $\{\text{Li}^+(\text{TEA})\}_2$ dimers interconnected by dihydrogen bonds between the OH groups from TEA and hydridic hydrogens from BH_4^- anions, forming one-dimensional extended ribbons. A total of ten $\text{H}\cdots\text{H}$ short contacts are present, six from one BH_4^- and four from another, with $\text{H}-\text{H}$ contact distances ranging between 1.62 and 2.28 Å. The smallest two distances of 1.62 and 1.67 Å represent the shortest $\text{H}\cdots\text{H}$ contacts reported so far for dihydrogen bonds. They appear to be the result of the strong complexation of the OH groups by the Li^+ cations, which in turn increases the acidity of the corresponding protons, as well as the solid-state reactivity of this system. The decomposition was induced thermally at 120 °C under an Ar atmosphere. In about 1 h the complex was completely decomposed, with the formation of an insoluble refractory material. On the basis of the crystal structure of **1**, the finding that 3 mol of H_2 were lost per mole of initial complex (on the basis of chemical analysis and TGA), and the solid-state ^{11}B MAS NMR spectrum, which showed a single peak at $\delta -4.6$ ppm (relative to $\text{B}(\text{OH})_3$), we proposed a one-dimensional polymeric trialkoxyborohydride structure for the final decomposed covalent product (**2**) (Figure 1). The formation of **2** appears to be topochemical, since a polymeric borate and unconverted LiBH_4 resulted from decomposition in DMSO solution. This outcome is not unexpected, as the intermediate $\text{BH}_x(\text{OR})_{4-x}^-$ species are usually more reactive than BH_4^- , and prone to disproportionation. What is surprising is that between the IR spectrum of **1** and **2**, the ν_{BH} differs significantly (Table 1). For reference, ν_{BH} for $\text{BH}(\text{OCH}_3)_3^-$ and BH_4^- are very similar in THF (2210 and 2220 cm^{-1} , respectively, for Li^+)^{9a} and virtually identical in the solid state (2250 cm^{-1} for Na^+),^{9b} and we found the same similarity between $\text{NaBH}_4\cdot\text{TEA}$ and its trialkoxyborohydride decomposi-

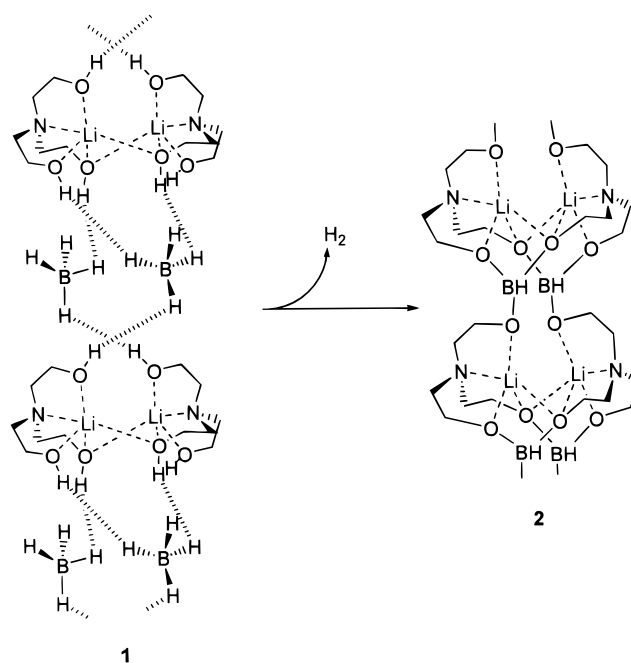


Figure 1. Schematic representation of the topochemical decomposition of **1** to the proposed trialkoxyborohydride **2**. The five most significant $\text{H}\cdots\text{H}$ interactions are illustrated.

Table 1. IR Data for $\text{LiBH}_4\cdot\text{TEA}$ (**1**), $\text{LiBD}_4\cdot\text{TEA}$ (**1a**), $\text{LiBH}_4(50\% \text{D})\cdot\text{TEA}$ (**1b**), and Their Corresponding Solid-State Decomposition Products, **2**, **2a**, and **2b** (LiBH_4 is included for comparison)

		IR $\nu_{\text{BH(BD)}} (\text{cm}^{-1})$
1		2231, 2290, 2369
2	initial	2171, 2247, 2301
	annealed	2340, 2368
1a		1652, 1704
2a	initial	1656
	annealed	1615 ^a
1b		1649, 1703, 1752
		2226, 2292, 2384
2b	initial	1656
		2169, 2247, 2291
	annealed	1613 ^a
		2340, 2369
LiBH₄		2219, 2301, 2378

^a Uncertain value due to the low intensity of the absorption and overlap with other vibration modes.

tion product.^{8a} However, theoretical calculations at the RHF/6-31G* level predict a significant red shift in the ν_{BH} when going from BH_4^- (2362 cm^{-1}) to $\text{BH}(\text{OCH}_3)_3^-$ (2190 cm^{-1}). On the other hand, the solid-state ^7Li MAS NMR chemical shifts for **2** and **1** are almost identical (Table 2).

As depicted in Figure 1, pairs of trialkoxyborohydrides are presumably present in **2**. Disproportionation into dialkoxyborohydride and borate is therefore conceivable in principle. For instance, in $\text{LiBH}(\text{OCH}_3)_3$, slow disproportionation into $\text{LiBH}_2(\text{OCH}_3)_2$ and $\text{LiB}(\text{OCH}_3)_4$ was observed in THF.^{9a,10} Table 2 presents the experimental ^{11}B NMR chemical shifts for the $\text{BH}_x(\text{OCH}_3)_{4-x}^-$ ($x = 0-4$) anions, for comparison with the experimental data found for **2**. Unfortunately, we did not find any NMR data in the literature referring to $\text{BH}_2(\text{OCH}_3)_2^-$. We therefore calculated the ^{11}B NMR chemical shifts for the same series at the RHF/6-31G* level (Table 2), finding good agreement between the experimental^{11,8a,b} and calculated values

(9) (a) Ashby, E. C.; Dobbs, F. R.; Hopkins, H. P. *J. Am. Chem. Soc.* **1975**, *97*, 3158. (b) Kadlec, V.; Hanzlik, J. *Collect. Czech. Chem. Commun.* **1974**, *39*, 3200.

(10) Brown, H. C.; Mead, E. J.; Shoaf, C. J. *J. Am. Chem. Soc.* **1956**, *78*, 3616.

Table 2. NMR Data for $\text{BH}_x(\text{OCH}_3)_{4-x}^-$, **1**, and **2**

	^{11}B NMR δ^a (ppm)		^7Li NMR δ^b (ppm)
	calcd	exptl	
BH_4^-	-50.7	-49.7 (solid) ^c -49.5 (solid) ^d	1.5 (solid LiBH_4) ^d
$\text{BH}_3(\text{OCH}_3)^-$	-26.4	-25.1 (THF) ^f	-
$\text{BH}_2(\text{OCH}_3)_2^-$	-12.8	-	-
$\text{BH}(\text{OCH}_3)_3^-$	-10.8	-8.6 (THF) ^f	-
$\text{B}(\text{OCH}_3)_4^-$	-14.9	-15.2 (CH_3OH) ^e -13.0 (THF) ^f	-
1	-	-48.0 (solid) ^d	2.8 (solid) ^d
2 , initial	-	-3.9 (solid)	3.1 (solid)
2 , annealed	-	-2.6 (solid)	1.0 (solid)

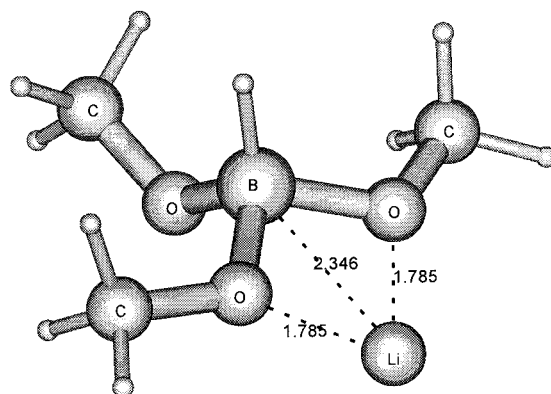
^a Relative to $\text{B}(\text{OCH}_3)_3$. ^b Relative to LiCl . ^c Reference 8a. ^d Reference 8b. ^e Reference 11a. ^f Reference 11b.

for the known $\text{BH}_x(\text{OCH}_3)_{4-x}^-$ anions. Compared to these values, however, our decomposed borohydrides exhibit δ values that are consistently shifted downfield. For example, decomposition of **1** or of its Na analogue in DMSO yielded polymeric borates which showed ^{11}B solid-state MAS NMR peaks at -5.2 and -4.3 ppm,¹² respectively, significantly different from the corresponding values in $\text{B}(\text{OCH}_3)_4^-$. Similarly, for a recently studied borate whose structure was confirmed by X-ray crystallography to be of the type $\text{B}(\text{OR})_3\text{OH}^-$, we obtained a δ value of -6.8 ppm,¹² which is again considerably different from the calculated value of -14.9 ppm in $\text{B}(\text{OCH}_3)_3\text{OH}^-$. However, for the solid-state decomposition product **2** and its Na analogue, we observed δ values of -3.9 and -6.4 ppm,¹² respectively, in better agreement with the corresponding experimental value of -8.6 ppm in $\text{BH}(\text{OCH}_3)_3^-$. The only possibilities that can be ruled out unambiguously based on the available data are the presence of $\text{BH}_3(\text{OR})^-$ or BH_4^- in **2**, which would display distinctive chemical shifts around -26 or -50 ppm, respectively. The chemical shifts for the other alkoxyborohydride species are too close to each other for a safe conclusion to be drawn. It would be very difficult to distinguish, especially in the solid state, between a $\text{BH}(\text{OR})_3^-$ structure and a 1:1 mixture of $\text{BH}_2(\text{OR})_2^-$ and $\text{B}(\text{OR})_4^-$ that would result from disproportionation.

An experiment that would possibly differentiate between the two possibilities is to decompose a sample of **1** that contains 50% deuterated borohydride. If any disproportionation occurred during decomposition, mixed $\text{BHD}(\text{OR})_2^-$ species would result, which should display IR bands significantly different from those of $\text{BH}_2(\text{OR})_2^-$ and $\text{BD}_2(\text{OR})_2^-$. Ab initio calculations at the RHF/6-31G* level predict the BH and BD stretching frequencies in $\text{BHD}(\text{OR})_2^-$ to be shifted by -10 and -53 cm^{-1} , respectively, relative to the corresponding values in dialkoxyborohydride or -borodeuteride, respectively. We first synthesized the reference $\text{LiBD}_4\cdot\text{TEA}$ (**1a**). The solid-state decomposition product resulting from this material (**2a**) exhibits the ν_{BD} at 48 cm^{-1} lower than the starting compound **1a** (Table 1). This change is comparable with the corresponding shift of -43 cm^{-1} accompanying the **1** to **2** transformation. We then obtained the 50% deuterated complex (**1b**), starting from a 1:1 mixture of LiBH_4 and LiBD_4 in THF, by precipitation with TEA. It exhibits ν_{BH} and ν_{BD} values that are very similar to the corresponding values in **1** and **1a** (Table 1). The IR spectrum of its solid-state decomposition product (**2b**) is virtually identical with the spectrum obtained by addition of the spectra corresponding to **2** and **2a** (Table 1). This result suggests that no disproportionation

(11) (a) Onak, T. P.; Landesman, H.; Williams, R. E.; Shapiro, I. J. *Phys. Chem.* **1959**, *63*, 1533. (b) Golden, J. H.; Schreier, C.; Singaram, B.; Williamson, S. M. *Inorg. Chem.* **1992**, *31*, 1533.

(12) Corrected by $+0.7$ ppm for adjustment to the $\text{B}(\text{OCH}_3)_3$ reference.^{11a}

**Figure 2.** Structure of $\text{LiBH}(\text{OCH}_3)_3$ optimized at the RHF/6-31G* level, with the interatomic distances in Å.

occurs during the solid-state decomposition of **1**, as a result of the isolation and reduced mobility of the borohydride units in **1** and **2**.

The X-ray powder pattern of **2** exhibits two broad peaks, indicating some degree of long-range order.^{8b} We attempted to enhance the crystallinity of this material by annealing at 120 $^\circ\text{C}$ under Ar. This process, however, induced a decrease in the XRD peaks of **2**, until they completely disappeared after approximately 2 weeks.¹³ While the hydridic content remained unchanged (one H^-), the ^{11}B and ^7Li MAS NMR chemical shifts moved 1.3 and 2.1 ppm downfield and upfield, respectively (Table 2). These changes point up the metastable nature of this topochemically controlled product. Moreover, the appearance of the BH stretching region in the IR spectrum changed considerably (Table 1) and apparently irreversibly, as the BH stretching absorptions did not revert to the original values even after 8 months at room temperature. A ν_{BH} shift to shorter wavelengths in metal borohydrides generally indicates a stronger $\text{BH}^-\cdots\text{M}^+$ interaction,¹⁴ and therefore a similar situation could be present in **2**. The observed shifts in the solid-state ^{11}B and ^7Li MAS NMR spectra are in agreement with this supposition. On the other hand, no disproportionation seems to have occurred, since again the IR spectrum of annealed **2b** is basically a summation of the corresponding spectra for **2** and **2a** (Table 1). The result of a topochemical reaction, the structure of **2** was very likely controlled by kinetic factors, and its subsequent annealing presumably allowed structural relaxation into a thermodynamically more stable arrangement in which the oppositely charged $\text{BH}(\text{OR})_3^-$ and Li^+ units are closer in space. The profound modifications in the IR spectrum of **2** and the relatively small downfield shift in its ^{11}B NMR spectrum are in good qualitative agreement with a $\text{BH}(\text{OCH}_3)_3^-\cdots\text{Li}^+$ model, whose optimized structure at the RHF/6-31G* level is shown in Figure 2. Its ν_{BH} frequency (scaled by 0.97)¹⁵ is estimated at 2418 cm^{-1} , comparable with the 2368 cm^{-1} value found in **2** after annealing. The ^{11}B NMR δ value of -10.7 ppm calculated for this model structure is virtually identical with the corresponding value in $\text{BH}(\text{OCH}_3)_3^-$, predicting that the above-mentioned interaction with Li^+ should have minimal influence over the ^{11}B NMR chemical shift.

B. Mechanistic Study. There are a few fundamental issues to be considered regarding the mechanism of the topochemical

(13) This transformation occurs faster (~ 4 days) if **2** is heated as a suspension in DMSO.

(14) (a) Price, W. C. *J. Chem. Phys.* **1949**, *17*, 1044. (b) Volkov, V. V.; Sobolev, E. V.; Grankina, Z. A.; Kalinina, I. S. *Russ. J. Inorg. Chem.* **1968**, *13*, 343. (c) Marks, T. J.; Kennelly, W. J.; Kolb, J. R.; Shimp, L. A. *Inorg. Chem.* **1972**, *11*, 2540.

(15) This scaling factor was obtained by comparison of the theoretical and experimental values of the strongest absorption in BH_4^- .

decomposition of **1** in particular, and of dihydrogen-bonded complexes in general. As for many other solid-state reactions, conventional concepts such as concentration, reaction order, or molecularity have little applicability here. More relevant in this context are the appearance and morphological evolution of the product phase, as well as its compatibility and "solubility" in the reactant phase.¹⁶ As thermally initiated solid-state reactions that yield both solid and gaseous products, decompositions of **1** (and other dihydrogen-bonded systems) are complex processes involving not only chemical steps such as breaking and formation of bonds but also physical transformations such as destruction of the initial lattice, reactant/product solid solution formation (with possible separation of the product phase), diffusion and desorption of H₂, and heat transfer.^{16,17} The variations in the crystals' morphology are of particular interest as they can provide critical information about the mechanism of decomposition.^{16d,17} The mechanism of this solid-state decomposition at the molecular level is particularly relevant for the successful design of the next generation of dihydrogen-bonded systems, and also for a better understanding of such fundamental processes as proton transfer or covalent bond formation, extensively studied in the gas phase and solution, but considerably less in the solid state.

Figure 3 presents typical optical micrographs showing crystals of **1** at different stages of decomposition at 110 °C. The initial transparent crystals gradually become opaque as the reaction progresses toward completion, suggesting the separation of a new phase. There is no visible reaction front advancing through the crystal; instead, the process appears to start randomly and proceed uniformly in the crystal bulk. The size and morphology of the crystals remained virtually unchanged during decomposition, practically eliminating the possibility of melting. However, when decomposition was examined with polarized light, a gradual disappearance of crystallinity could be observed.

When decomposition of **1** was monitored in situ by ¹¹B solid-state MAS NMR spectroscopy, no other boron species than the initial BH₄⁻ and the final trialkoxyborohydride could be detected, probably because of the increased reactivity and the short lifetime of the intermediate mono- and dialkoxyborohydrides. Integration of the two well-separated peaks proved to be a suitable way to measure the extent of the solid-state decomposition, and thus to study the kinetics of this topochemical reaction independent of other physical transformations that occur during the process. We studied the solid-state decomposition of **1** at temperatures between 105 and 120 °C, using LiBH₄·TEA samples from the same batch for each experiment to eliminate any possible error introduced by sample variation.¹⁸ The resulting conversion–time curves (Figure 4) have the typical sigmoid shape characteristic for most solid-state decompositions of the type A_{solid} → B_{solid} + C_{gas}.^{16,17} The short initiation period is followed by a rapid increase in reaction rate

(16) (a) Hannay, N. B. *Reactivity of Solids*; Treatise On Solid State Chemistry; Plenum Press: New York, 1976; Vol 4. (b) Curtin, D. Y.; Paul, I. C.; Duesler, E. N.; Lewis, T. W.; Mann, B. J.; Shiau, W. I. *Mol. Cryst. Liq. Cryst.* **1979**, *50*, 25. (c) Paul, I. C.; Curtin, D. Y. *Acc. Chem. Res.* **1973**, *6*, 217. (d) Galwey, A. K. *Pure Appl. Chem.* **1995**, *67*, 1809. (e) Dunitz, J. D. *Acta Crystallogr.* **1995**, *B51*, 619. (f) Vyazovkin, S.; Wight, C. A. *Annu. Rev. Phys. Chem.* **1997**, *48*, 125. (g) Vyazovkin, S.; Wight, C. A. *J. Phys. Chem. A* **1997**, *101*, 8279. (h) Epple, M.; Troger, L. *J. Chem. Soc., Dalton Trans.* **1996**, 11. (i) Shin, S. H.; Cizmeciyan, D.; Keating, A. E.; Khan, S. I.; Garcia-Garibay, M. A. *J. Am. Chem. Soc.* **1997**, *119*, 1859.

(17) (a) Sekiguchi, K.; Shirotani, K.-I.; Sakata, O.; Suzuki, E. *Chem. Pharm. Bull.* **1984**, *32*, 1558. (b) Tanaka, H.; Koga, N. *J. Phys. Chem.* **1988**, *92*, 7023. (c) Koga, N.; Tanaka, H. *J. Phys. Chem.* **1994**, *98*, 10521.

(18) We noticed a significant variation in decomposition rates among different samples, a feature characteristic of many solid-state reactions.^{16,17} See also: Brill, T. B.; Gongwer, P. E.; Williams, G. K. *J. Phys. Chem.* **1994**, *98*, 12242.

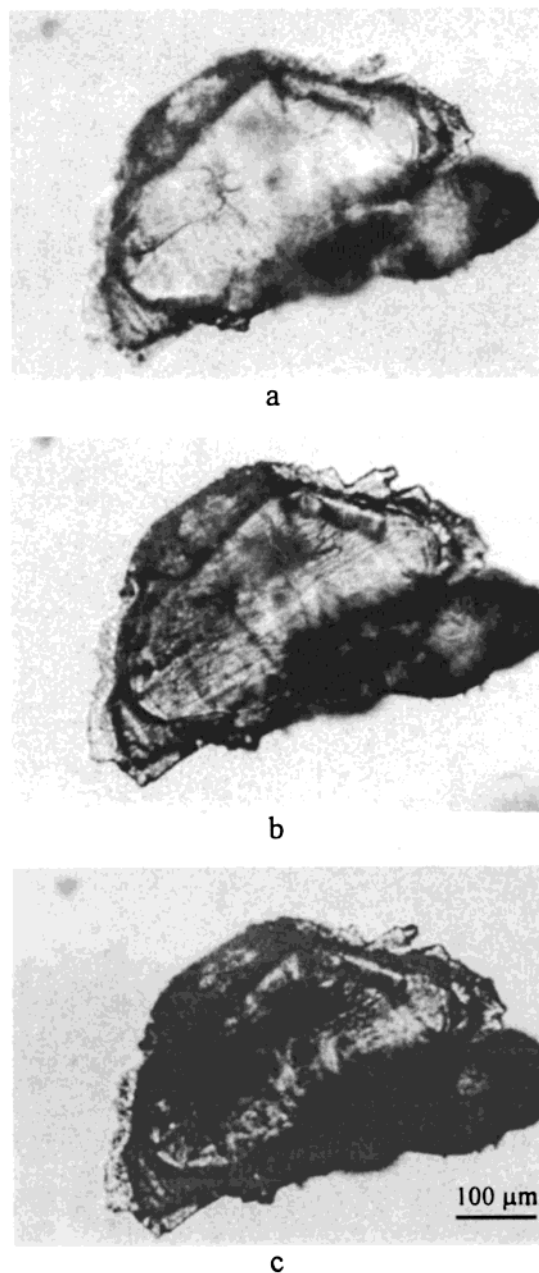


Figure 3. Typical microscopic view (transmitted light) of LiBH₄·TEA solid-state decomposition: (a) initial crystal, (b) 10 min at 110 °C, and (c) final decomposed crystal. Scale bar: 100 μm.

up to the inflection point, after which time the rate decreases monotonically to zero. This pattern is almost universally associated with the initiation of reaction at specific sites followed by the growth of nuclei, with the reaction mostly confined to the product/reactant interface. The kinetics is therefore controlled by the number of nuclei present and the total area of the expanding interface. After the inflection point, the growing nuclei start to coalesce, slowing the decomposition rate as the interfacial area decreases, until the reaction eventually stops.

Different kinetic models with their corresponding equations have been elaborated to account for various solid-state decomposition mechanisms. Among them, the most common are the Avrami–Erofeyev equation (eq 1) and the phase boundary model (eq 2).^{16,17}

$$[-\ln(1 - \alpha)]^{1/n} = kt; \quad n = 1-4 \quad (1)$$

$$1 - (1 - \alpha)^{1/n} = kt; \quad n = 1-3 \quad (2)$$

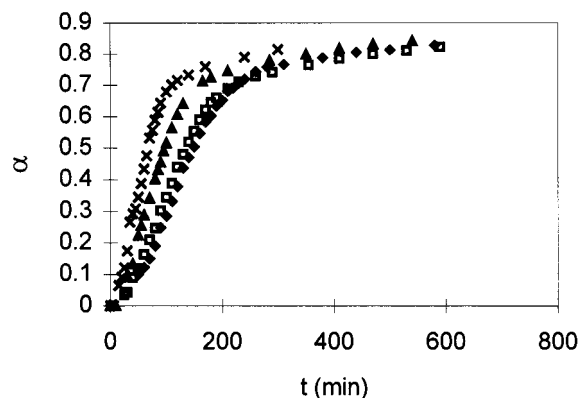


Figure 4. Conversion (α) vs time curves for the solid-state decomposition of **1**: \blacklozenge , 105 °C; \square , 110 °C; \blacktriangle , 115 °C; \times , 120 °C.

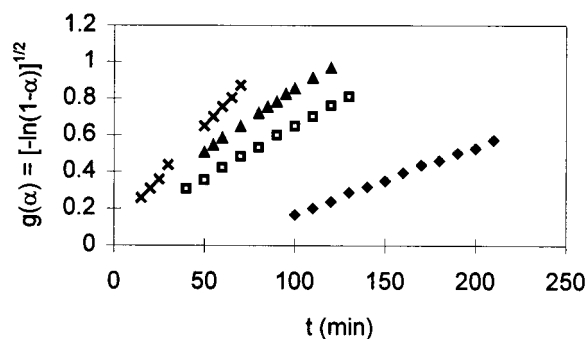


Figure 5. Plots of the Avrami–Erofeyev law, $[-\ln(1-\alpha)]^{1/2}$, against time for the solid-state decomposition of **1**: \blacklozenge , 105 °C; \square , 110 °C; \blacktriangle , 115 °C; \times , 120 °C.

Table 3. Rate Constants k for the Solid-State Decomposition of **1**, Calculated from the Avrami–Erofeyev Law for Nucleation and Two-Dimensional Growth in the Specified Conversion Ranges, Together with the Correlation Coefficients of the Linear Regression Analysis R^2

temp (°C)	k (min ⁻¹) $\times 10^4$	conversion range	R^2
105	37 ± 1.4	0.284–0.681	0.9980
110	56 ± 2.6	0.090–0.480	0.9988
115	66 ± 2.8	0.224–0.606	0.9979
120	111 ± 0.9	0.064–0.531	0.9990

The first one corresponds to a nucleation and growth mechanism, while the second is associated with an inward advancement of the reaction interface from the crystal's edges. It should be pointed out, however, that very often there is no single model that can acceptably describe the whole conversion range, as different mechanisms may operate for different stages of decomposition. The agreement of our data to eqs 1 and 2 as well as to other models for solid-state decompositions^{16,17} was compared, and the best match was found for a nucleation and two-dimensional growth mechanism. The corresponding plots of $[-\ln(1-\alpha)]^{1/2}$ against time for different temperatures studied are presented (Figure 5), together with the obtained rate constants k , the correlation coefficients of the linear regression analysis R^2 , and the conversion ranges for which the Avrami–Erofeyev law is obeyed (Table 3). It could be speculated that the two-dimensional expansion of nuclei might originate in the crystal structure of **1**, consisting of one-dimensional dihydrogen-bonded ribbons linked by conventional H-bonds in overall extended layers. Once decomposition has started, it is more likely it will propagate within the same layer, where the H-bonding network is disrupted, weakening thus the compactness of the crystalline environment. By comparison, a similar mechanism, but with a three-dimensional growth of nuclei (n

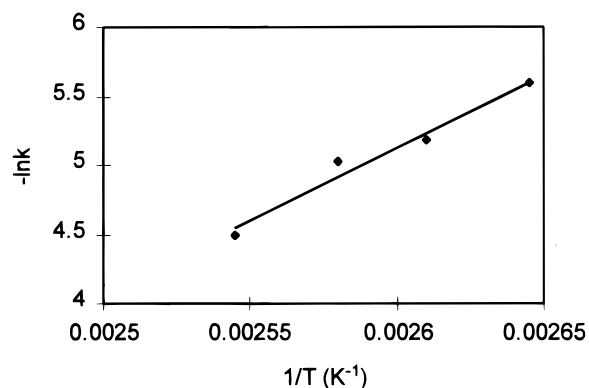


Figure 6. Arrhenius plot for the solid-state decomposition of **1** at 105–120 °C.

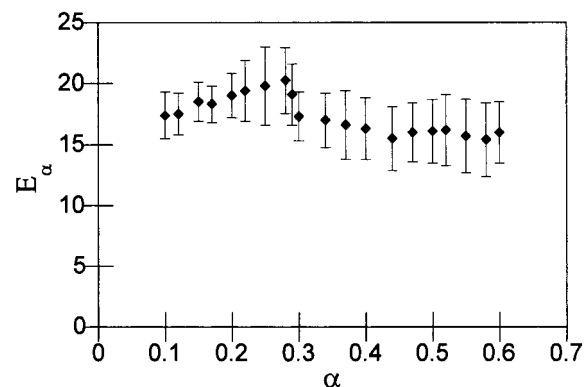


Figure 7. Variation of activation energy with conversion for the solid-state decomposition of **1**, obtained using the isoconversional method.

= 3), gave a worse match (av $R^2 = 0.9852$ vs 0.9984 for $n = 2$). For the late stages of decomposition, however, although the 2D or 3D contraction mechanisms (eq 2) fit somewhat better than other decomposition models, they do not provide an acceptable description of our data.

The measured rate constants for the solid-state decomposition of **1** at temperatures between 105 and 120 °C¹⁹ obey the Arrhenius equation ($R^2 = 0.9755$), as illustrated by the linear dependence of $\log k$ against $1/T$ (Figure 6). An activation energy of 21.0 ± 2.4 kcal/mol for the solid-state decomposition of **1** can be estimated from our data. Similarly, using the Eyring equation, the activation parameters for decomposition, ΔH^\ddagger and ΔS^\ddagger , were calculated to be 20.1 ± 2.4 kcal/mol and -16.8 ± 6.2 eu, respectively.

An alternative approach for the kinetic analysis of solid-state reactions is the isoconversional method, applied under isothermal or nonisothermal conditions.^{16f,g} This strategy allows the estimation of the activation energy without assuming a particular reaction model, and is particularly convenient for analysis of nonisothermal data such as that obtained from DSC and TGA experiments. Under isothermal regime, the activation energy at a particular conversion, E_{α} , can be evaluated using eq 3:^{16g}

$$-\ln t_{\alpha,i} = \ln[A/g(\alpha)] - E_{\alpha}/RT_i \quad (3)$$

The major disadvantage of this method, however, is that the obtained activation energy varies significantly with the extent

(19) At temperatures above 120 °C, the solid-state decomposition of **1** becomes faster than predicted by the Arrhenius equation. A possible explanation is that the dissipation of the resulting heat becomes too slow compared to decomposition rate, eventually leading to the autoacceleration of reaction. No melting occurs even under these conditions, as verified by optical microscopy.

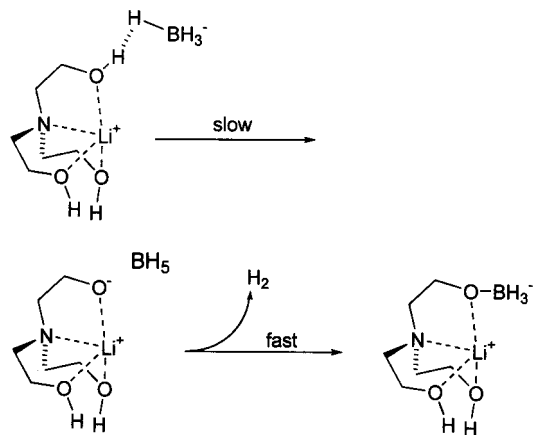


Figure 8. Proposed mechanism for the first B-H...H-O to B-O topochemical conversion in **1**.

of reaction, which complicates the interpretation of the kinetic data.^{16f} We applied eq 3 to our data, and the resulting E_{α} versus α plot is illustrated in Figure 7. The activation energies thus obtained are, within experimental errors, generally comparable with the value calculated using the model-fitting method.²⁰

Since the kinetic measurements were done by in situ ¹¹B NMR spectroscopy, which allowed direct monitoring of the appearance of the final trialkoxyborohydride product, independent of other physical processes such as nucleation, phase separation, or diffusion and desorption of H₂, and considering the fact that no phase transition occurred prior to decomposition, as shown by powder X-ray diffraction, it is reasonable to assume that the kinetic parameters found in this study are directly related to the chemical transformations responsible for decomposition.²¹ Moreover, the present activation parameters are comparable with the activation enthalpy of 20.6 ± 1 kcal/mol and activation entropy of -22.3 ± 3 eu found for the hydrolysis of BH₄⁻ in neutral water, and associated with the rate-limiting proton-transfer step.²² However, the mechanism could be different in the solid state, with the H₂ evolution slowed by the crystal constraints, possibly becoming the rate-determining step. To address this question, we studied the solid-state decomposition of LiBH₄·N(CH₂CH₂OD)₃, the analogue of **1**, with the OH groups deuterated. H/D exchange between BH₄⁻ and OD groups of the TEA is expected for a scheme involving fast, reversible proton transfer followed by slow H₂ loss. However, no H/D exchange was observed at any stage of decomposition, under various conditions, as indicated by the IR or ¹H NMR of the partly or fully decomposed deuterated complex. This experiment suggests that as in solution, the proton transfer is slow compared to H₂ loss and B–O covalent bond formation (Figure 7).²³ The measured activation parameters for the solid-state decomposition of **1** can therefore be associated with the proton transfer at the

(20) Analyses starting with $t_{0,i}$ initial times set at various extents of reaction, α , yield different E_{α} values. For instance, when $t_{0,i}$ is set for $\alpha = 0.1$, the resulting activation energies vary between 14.9 and 24.1 kcal/mol. In comparison, the Avrami–Erofev (n = 2) model analysis does not show much variation. Considering also the fact that it fits our data much better than any other model, and is in agreement with the microscopic observations and available structural data for **1**, we think that the use of this model is particularly appropriate for the present study.

(21) For other solid-state reactions where the kinetics are directly coupled to chemical transformations see, for example: (a) Galwey, A. K.; Mohamed, M. A. *J. Chem. Soc., Faraday Trans.* **1985**, *81*, 2503. (b) Son, S. F.; Asay, B. W.; Henson, B. F.; Sander, R. K.; Ali, A. N.; Zielinski, P. M.; Phillips, D. S.; Schwarz, R. B.; Skidmore, C. B. *J. Phys. Chem. B* **1999**, *103*, 5434.

(22) These values were obtained using OH⁻ concentration data. When pH data were used, slightly different values were obtained: $\Delta H^{\ddagger} = 22.1 \pm 1$ kcal/mol; $\Delta S^{\ddagger} = -18.4 \pm 3$ eu. See: Mesmer, R. E.; Jolly, W. L. *Inorg. Chem.* **1962**, *1*, 608.

reaction interface. The reacting partners in this region are presumably more flexible than in the perfectly ordered environment of the undisturbed crystal. The lower activation entropy found for this process, compared to the similar reaction in water, could be attributed to the preorganization imposed by the dihydrogen bonding network in the crystal. Despite the heterogeneous nature of decomposition, the topochemical information is nonetheless transferred through the interface, to the newly formed covalent product.²⁴

Conclusions

Solid-state decomposition of the dihydrogen-bonded LiBH₄·TEA complex was investigated using IR and in situ solid-state ¹¹B MAS NMR spectroscopies, optical microscopy, XRD, and chemical analysis. After the initial topochemical loss of 3 mol of H₂ with the formation of a polymeric trialkoxyborohydride covalent material, subsequent annealing at 120 °C induced additional structural modifications associated with the complete disappearance of order, apparently accompanied by the migration of Li⁺ cations into closer proximity to the negatively charged BH(OR)₃⁻ centers. Both the microscopic examination and the kinetics of decomposition indicate a heterogeneous process with phase separation of the resulting covalent material. A mechanism involving random nucleation followed by two-dimensional growth of nuclei best fit the observed conversion–time data.²⁵ The measured rate constants at temperatures between 105 and 120 °C obey the Arrhenius law, and an activation energy of 21.0 ± 2.4 kcal/mol was found for decomposition. The estimated activation parameters, ΔH^{\ddagger} and ΔS^{\ddagger} , of 20.1 ± 2.4 kcal/mol and -16.8 ± 6.2 eu, respectively, are comparable with the corresponding values reported for the neutral aqueous hydrolysis of BH₄⁻, suggesting similar decomposition mechanisms in solution and solid state. To all appearances, these activation parameters correspond to rate-limiting proton transfer at the interface between the crystalline dihydrogen-bonded system **1** and the newly formed covalent product **2**.

In summary, we have reported the first detailed mechanistic study of a topochemical dihydrogen to covalent bonding transformation. More dihydrogen-bonded systems and their solid-state decompositions need to be studied to probe the generality of this analysis, and we continue to pursue this fascinating subject, which adds new dimensions to the expanding field of supramolecular chemistry, by building a bridge between molecular crystals, self-assembled by weak intermolecular interactions, and extended, ordered covalent solids.

(23) We interpret our results using a stepwise mechanism for the solid-state decomposition based on analogy with the aqueous hydrolysis of BH₄⁻ in neutral water, and theoretical calculations supporting the existence of the BH₅ intermediate (see, for example: Schreiner, P. R.; Schaefer, H. F., III; Schleyer, P. v. R. *J. Chem. Phys.* **1994**, *101*, 7625). In the solution the four-center transition state could be unambiguously eliminated based on kinetic isotope effects and hydrolysis experiments in the presence of trimethylammonium ion (Davis, R. E. *J. Am. Chem. Soc.* **1962**, *84*, 892), but in our solid-state system the possibility of a concerted mechanism cannot be ruled out. However, considering the similarity of the reacting partners and the activation parameters found in our study and in solution, it appears the same mechanism should apply for both.

(24) Analysis of a great number of solid-state reactions indicated that there is no strong correlation between the chemical specificity and the overall crystallographic order of the final solid phase. See: Gougoutas, J. Z. *Pure Appl. Chem.* **1971**, *27*, 305.

(25) Neither our failure to observe reaction fronts nor the fact that the random nucleation model gives the best fit to the data preclude the possibility that reaction is initiated at preexisting defects in the crystal. Indeed, the observed sample-dependent variation in absolute rate of decomposition¹⁸ may support the latter suggestion.

Experimental Section

FT-IR spectra were measured in KBr pellets on a Perkin-Elmer Spectrum 2000 instrument. ^{11}B (128.33 MHz) and ^7Li (155.44 MHz) solid-state MAS NMR spectra were recorded on a Varian VXR-400 instrument, using solid boric acid and LiCl, respectively, as references; a negative sign represents a chemical shift upfield from reference. X-ray powder diffraction measurements were conducted on a Rigaku-Denki RW400F2 diffractometer with monochromatic Cu K α radiation, operated at 45 kV and 100 mA. Optical micrographs were obtained with a Nikon AFX-DX microscope equipped with a Mettler FP82HT hot stage. Analysis of the hydridic content was done by titration with diluted HCl and volumetric measurement of the H_2 evolved. TEA- d_3 was obtained by repeated dissolution of TEA in D_2O (99.9% D) followed by removal of the water at 85 °C under vacuum, until the ^1H NMR (DMSO- d_6) signal for the OH protons completely disappeared. LiBD_4 was synthesized by metathesis,²⁶ from NaBD_4 (98% D).

In Situ ^{11}B MAS Solid-State NMR. All spectra were recorded at a MAS frequency of 3.8 kHz, using 2.0 ms $\pi/2$ pulses, with a recycle delay of 5 s, to allow full relaxation of all boron species.²⁷ For each experiment, 48 scans were acquired. The observed spectra were deconvoluted into Lorentzian lines, and the ratios of the resulting integrals, corresponding to product and starting material, respectively, were used to estimate the extent of decomposition.

Theoretical Calculations. All calculations were carried out with the GAUSSIAN 98 package²⁸ at the RHF/6-31G* level. Each structure was fully optimized and confirmed by vibrational analysis to be a minimum on the potential energy surface.

LiBH_4 ·TEA- d_3 . A mixture of 0.22 g (10 mmol) of LiBH_4 and 1.4 mL (10.3 mmol) of TEA- d_3 in 30 mL of THF was stirred under Ar at room temperature for 1 h. The resulting precipitate was filtered and washed with THF. Yield: quantitative. ^1H NMR ($\text{CH}_3\text{CN}-d_3$): no OH signal. IR (KBr): $\nu_{\text{OD}} = 2516\text{ cm}^{-1}$. Anal. hydridic content: 4.06.

LiBD_4 ·TEA (1a). A mixture of 0.065 g (2.5 mmol) of LiBD_4 and 0.4 g (2.7 mmol) of TEA in 8 mL of THF was stirred under Ar at

room temperature for 2 h. The resulting precipitate was filtered and washed with THF. IR (KBr): $\nu_{\text{BD}} = 1704, 1652\text{ cm}^{-1}$. Anal. hydridic content: 3.90, 90% D based on ^1H NMR (DMSO- d_6).

LiBH_4 (50% D)·TEA (1b). A mixture of 0.044 g (2 mmol) of LiBH_4 and 0.052 g (2 mmol) of LiBD_4 was dissolved in 12 mL of THF. TEA (0.64 g, 4.3 mmol) was subsequently added and the mixture was stirred under Ar at room temperature for 2 h. The resulting precipitate was collected and washed with THF. IR (KBr): $\nu_{\text{BD}} = 1752, 1703, 1649\text{ cm}^{-1}$; $\nu_{\text{BH}} = 2384, 2292, 2226\text{ cm}^{-1}$. Anal. hydridic content: 3.80, 54% D based on ^1H NMR (DMSO- d_6).

H/D Isotope Exchange Experiments. Aliquots of 0.1–0.3 g of LiBH_4 ·TEA- d_3 were heated under dry Ar at 85–110 °C, monitoring the decompositions by H^- analysis. The partly or fully decomposed samples were analyzed by IR (KBr) and ^1H NMR ($\text{CH}_3\text{CN}-d_3$). No signals for the ν_{BD} in the IR or for OH in ^1H NMR spectra were observed throughout the reaction.

Acknowledgment. The support of the MSU Center for Fundamental Materials Research (Grant R508) is gratefully acknowledged. We thank Professor Gregory L. Baker for making available the hot stage microscope and Mr. Kermit M. Johnson for assistance with solid-state NMR.

JA994361U

(28) Frisch, M. J.; Trucks, G. W.; Schlegel, H. B.; Scuseria, G. E.; Robb, M. A.; Cheeseman, J. R.; Zakrzewski, V. G.; Montgomery, J. A.; Stratmann, R. E.; Burant, J. C.; Dapprich, S.; Millam, A. D.; Daniels, A. D.; Kudin, K. N.; Strain, M. C.; Farkas, O.; Thomas, J.; Barone, V.; Cossi, M.; Cammi, R.; Mennucci, B.; Pomelli, C.; Adamo, C.; Clifford, S.; Ochterski, J.; Petersson, G. A.; Ayala, P. Y.; Cui, Q.; Morokuma, K.; Malick, D. K.; Rabuck, A. D.; Raghavachari, K.; Foresman, J. B.; Cioslowski, J.; Ortiz, J. V.; Stefanov, B. B.; Liu, G.; Liashenko, A.; Piskorz, P.; Komaromi, I.; Gomperts, R.; Martin, R. L.; Fox, D. J.; Keith, T.; Al-Laham, M. A.; Peng, C. Y.; Nanayakkara, A.; Gonzalez, C.; Challacombe, M.; Gill, P. M. W.; Johnson, B. G.; Chen, W.; Wong, M. W.; Andres, J. L.; Head-Gordon, M.; Replogle, E. S.; Pople, J. A.; Gaussian, Inc.: Pittsburgh, PA, 1998.

(26) Schlesinger, H. I.; Brown, H. C.; Hyde, E. K. *J. Am. Chem. Soc.* **1953**, *75*, 209.

(27) Eckert, H. *Prog. Nucl. Magn. Reson. Sp.* **1992**, *24*, 159.